Oligoamide grafted with perfluoropolyether blocks: a potential protective coating for stone materials

Yijian Cao[a,b]; Antonella Salvini[b]; Mara Camaiti[a*]

[a] CNR-Institute of Geosciences and Earth Resources, Via Giorgio La Pira 4 - 50121, Florence, Italy, e-mail: yijian.cao@unifi.it;
[b] Department of Chemistry, University of Florence, Via della Lastruccia 3-13, 50019, Sesto Fiorentino (FI), Italy, e-mail: antonella.salvini@unifi.it.
* Corresponding author: mara.camaiti@igg.cnr.it; Via Giorgio La Pira, 4 - 50121 Florence (Italy); phone: +39-055-2757558.

Abstract

In order to mitigate the decay phenomena induced by liquid water adsorption and penetration, new protective coating agents with high hydrophobicity, photo-oxidative stability and good solubility in non-toxic solvents are needed. In the present study, a partially fluorinated oligoadipamide bearing pendant PFPE segments (FAD) together with two diamides i.e., ethylenediamide (DC2) and hexamethylenediamide (DC6) incorporating perfluoropolyether (PFPE) segments, were synthesized via condensation reactions. The diamides are only soluble in chlorofluorocarbons, while the oligoadipamide is soluble in alcohols and hydro-alcoholic solvents e.g., ethanol, 2-propanol. The polymerization degree, together with the molecular weight and molecular weight distribution of oligoethylene-adipamide evaluated by ^{1}H-NMR spectroscopy, was found very low which allowed to obtain a partially fluorinated amide with a high fluorine content (57%). To determine the protective performance of the new FAD, a series of standard tests were conducted on Lecce stone and Carrara marble samples. Regarding water repellence, compared with a commercial fluoroelastomer tested as a reference material, FAD demonstrated much higher water repellence when applied on Carrara marble samples, and comparable hydrophobic effect when applied on Lecce stone samples. In comparison with the two diamides, tested on Lecce stone, the oligoamide manifested similar protective efficacy with a much less amount applied (15 g/m^2 versus 154/150 g/m^2). In addition to its high hydrophobicity, FAD also preserved the original vapor permeability and chromatic features of coated surfaces. With these favorable properties, this new oligomeric product is ought to be proposed as protective coating material for stone heritage.

Key words: oligoadipamide; perfluoropolyethers; protective coating; stone artworks

1. Introduction

The survival of our mankind's stone heritage is challenged by severe, diverse degradation events that derive from environmental origins, anthropogenic and biological behaviors [1-6]. Among all deteriorating agents, liquid water has been regarded to take the highest responsibility for stone decay. Since water not only causes dissolution of binding media in stone, it also brings in atmospheric pollutants e.g., elemental carbon, carbonates, sulfur and nitrogen compounds, metallic particles which may promote the decay processes [3, 7]. Since ancient times, in order to prevent contact with extraneous deteriorating substances, especially polluted atmospheric water, a hydrophobic barrier film is commonly created on stone surfaces by applying natural or synthetic materials [8]. In modern times, synthetic products such as acrylic resins, silicon based resins and fluorinated polymers are very popular attributing to their good hydrophobicity, chemical compatibility, stability and in some cases, the ability of acting also as consolidation agents [9- 11]. Yet, they also show several drawbacks in long-term use. Acrylic polymers have poor photo-oxidative stability due to structural reasons,

while silicon based resins are reactive with some specific stones and may become insoluble after in-situ polymerization [12-16].

Fluorinated polymers, particularly perfluoropolyethers (PFPE) (Scheme 1) and their derivatives have been suggested and applied as water repellents for stone conservation since 1980s [17-19].

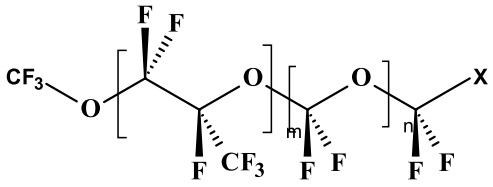

Scheme 1

where X= $-CF_3$ (named YR), -COOH, $-COOCH_2-CH-(CH_2)_2$, $-CONH-CH_2-CH-(CH_2)_2$ (named IBA).

Owing to high bond energy of C-F bond and to highly electronegative fluorine atoms, PFPEs possess high hydrophobicity, high chemical, thermal and photo-oxidative stability. Fomblin YR®, the non-functionalized oil (X= $-CF_3$ in scheme 1), derived from photo-oxidation of hexafluoropropene, was the first PFPE compound used for stone protection [17]. However, it has poor adhesion to stone substrates, which is insufficient to maintain the oil in place, leading to surface migration or absorption by the porous substrate. This phenomenon results from the inadequate intermolecular interaction provided by the lone pair of electrons on oxygen atoms. As a consequence, the treatment efficacy (hydrophobic properties) decreases dramatically with time. Later, a significant improvement in application was accomplished by introducing functional derivatives of PFPEs, among which the amide derivatives (IBA in Scheme 1 and DC6) have manifested the best performances [18, 19]. The problem of poor adhesion was addressed, and satisfying protective effects were achieved. Whereas, the limited solubility of mono- or di-amide in chlorofluorocarbons (CFCs), i.e. 1,2,2-trichloro-1,1,2 trifluoroethane (A113) has retarded their wide application, since CFCs have been banded worldwide for inducing ozone depletion. Eligible protective materials for artworks are required to have good solubility in non-toxic, environmentally benign solvents.

Considering the basic requirements of protective treatments on artifacts and the limitations of commercial materials available on market, new products that integrate high hydrophobicity, stability and good solubility in non-toxic solvents are urgently needed. Recently, innovative hybrid nanocomposites based on boehmite nano-particles and methacrylic-siloxane monomers were proposed as protective coatings for carbonate stones [20,21]. Though these new materials showed promising properties, mainly in terms of hydrophobicity, vapor permeability, and durability to weathering agents, their expected insolubility after curing may compromise the reversibility of the treatment. Moreover, the chromatic changes of the treated surfaces do not always fulfill the requirements of cultural heritage conservation. We herein report the synthesis, characterization and testing of a new oligoamide bearing pendant PFPE segments

which has good solubility in alcohol and hydro-alcoholic solvents (e.g., ethanol, 2-propanol), also after application on stone substrates (reversible treatment). A series of standard tests were carried out, and satisfactory results were obtained by comparing its performance with those of a commercial fluoroelastomer (N215) and other low molecular weight PFPE bearing diamides, such as DC2 and DC6. In addition to endowing high hydrophobicity, the new oligoamide also preserves the original vapor permeability and chromatic features of coated stone substrates.

2. Experimental

2.1 Chemicals

Ethylenediamine (>99.5%) (C2) was purchased from Fluka. Diethyl adipate (99%) and hexamethylendiamine (>98%) (C6) were purchased from Sigma-Aldrich. Absolute ethanol, acetone and anhydrous diethyl ether are products of J. T. Baker. 2- Propanol (>99.5%) was purchased from EMSURE. Galden acid (monocarboxylic acid of PFPE with M_n≈900) and 1,2,2-trichloro-1,1,2 trifluoroethane (A113) were kindly supplied by Ausimont S.p.A. Fluoroelastomer (poly hexafluoropropene-*co*-vinylidene fluoride, Mw≈125,000) (N215) was kindly supplied by Solvay Solexis-Milan. A113 was distilled before use, while all the other chemicals were used as received without further purification.

Methyl and ethyl esters of Galden acid were prepared by esterifying the Galden acid with absolute methanol/ethanol prior to use. The average molecular weight was determined by alkali titration. The esters were prepared by heating the acid with alcohols in excess, removing the azeotropic mixture water-alcohol formed continuously by rectification [18].

The syntheses of amides were carried out under nitrogen atmosphere using standard Schlenk line techniques. The kinetics of all reactions was monitored by FT-IR spectroscopy at regular intervals till completion. The final products were characterized by FT-IR and NMR spectroscopy (^{1}H, ^{19}F).

2.2 Synthesis of partially fluorinated oligoadipamide

2.2.1 Synthesis of oligoadipamide (ADC2)

In a two-necked 100 ml flask, equipped with a reflux condenser and a dropping funnel, ethylenediamine (1.429 ml, 24.75 mmol) was introduced under nitrogen. Under vigorous stirring, diethyl adipate (1 g, 0.9911 ml, 4.95 mmol) was then added dropwise through the funnel. The flask was placed in an oil bath for reaction at 95 °C for 22 hours. The resulting yellowish precipitate was washed with 10 ml of diethyl ether for 3 times and concentrated under vacuum. The product recovered was white solid (0.897g, yield 61%). The product was characterized by FT-IR spectroscopy (Table 1), ^{1}H-NMR and ^{13}C-NMR spectroscopy (Table 2), and the number-average molecular weight was estimated by ^{1}H-NMR spectroscopy as well

2.2.2 Synthesis of partially fluorinated oligoadipamide (FAD)

The same reaction apparatus for oligoamides synthesis was adopted. In a two-necked 100 ml flask, 2-propanol (5 ml) was added to the oligoadipamide (0.15 g, 0.5065 mmol) under vigorous stirring. After formation of colloidal solution, ethyl ester of Galden acid (0.894g, 1.016 mmol) in 2 ml of A113 was introduced dropwise through dropping funnel. 3 ml of 2-propanol was added lastly in order to wash the dropping funnel. The mixture was stirred for 20 hours at room temperature. The flask was then placed in an oil bath for reaction at 65 °C for 40 hours. The white precipitate formed at room temperature was partially dissolved when the mixture was heated. After solvent evaporation under reduced pressure and purification with 5 ml of A113 for 3 times, 0.941 g (yield 95%) of slightly yellowish, waxy product was recovered. The product was further characterized by FT-IR spectroscopy (Table 1) and ^{19}F-NMR spectroscopy (Table 3).

2.2.3 Synthesis of hexamethylenediamide (DC6) /ethylenediamide (DC2) of Galden acid

In accordance to [18], the same reaction set-up and procedures were used for the syntheses of the two diamides. The synthesis of hexamethylenediamide was described as a typical example.

In a two-necked 100 ml flask, equipped with a reflux condenser and a dropping funnel, hexamethylenediamine (0.49 g, 4.2 mmol) in 10 ml of A113 was introduced under nitrogen. The methyl ester of Galden acid (7.7 g, 8.5 mmol) was then added slowly under nitrogen atmosphere and moderate stirring, through the dropping funnel. The reaction completed in 6 hours at room temperature. 7.7 g of yellowish material was recovered after solvent distillation at reduced pressure. The raw product was then treated with active carbon in 10 ml of A113. At last, 7.4 g (yield 95%) of oily, dense, colorless and transparent product was obtained after filtration (filter ranging from 8 to 0.8 microns), washing again with A113 and evaporation of solvent at reduced pressure. The final product was characterized by FT-IR spectroscopy (Table 1), ^{1}H-NMR and ^{19}F-NMR spectroscopy (Tables 2 and 3). Meanwhile, ethylenediamide with PFPE segments (DC2) was characterized by FT-IR spectroscopy (Table 1),^{1}H-NMR and ^{19}F-NMR spectroscopy (Tables 2 and 3) as well.

Table 1 Main absorptions of the FT-IR spectrum of the synthesized products

* The spectrum was acquired in diamond anvil cell; ^ The spectrum was acquired between KBr windows

Product	Absorption (cm^{-1})					
	ν_{N-H}	ν_{C-H}	$\nu_{C=O}$	δ_{N-H}	ν_{C-N}	ν_{C-F}
ADC2*	3295 3082	2938 2857	1637	1554	1441	
FAD*	3296 3089	2949	1705 ($\nu_{Rf-C=O)}$ 1641	1559	1440	1400-900
DC6^	3315 3100	2944 2866	1708 ($\nu_{Rf-C=O)}$	1553	1444	1400-900
DC2^	3318 3107	2956 2881	1707 ($\nu_{Rf-C=O)}$	1553	1441	1400-900

Table 2 Characteristic ^{1}H-NMR and ^{13}C-NMR chemical shifts of the synthesized products

Product	^{1}H-NMR chemical shifts (ppm)								
	-NH-C<u>H</u>$_2$-C<u>H</u>$_2$-NH-	H$_2$N-CH$_2$-C<u>H</u>$_2$-	H$_2$N-C<u>H</u>$_2$-	-NH-CO-C<u>H</u>$_2$-	-CH$_2$-C<u>H</u>$_2$-C<u>H</u>$_2$-CH$_2$-	-CO-N<u>H</u>-	-CO-NH-C<u>H</u>$_2$-	-CH$_2$-C<u>H</u>$_2$-CH$_2$-	-CH$_2$-C<u>H</u>$_2$-C<u>H</u>$_2$-CH$_2$-
ADC2*	3.27 (s, 4H)	3.20 (t,2H) ($J_{H\text{-}H}$ = 6.2 Hz)	2.64 (t,2H) ($J_{H\text{-}H}$ = 6.2 Hz)	2.23 (s, 2H)	1.54 (s, 4H)				
DC6^						7.51 (s, 1H)	3.36 (s, 2H)	1.61 (s, 2H)	1.40 (s, 4H)
DC2^	3.58 (s, 4H)					8.39 (s, 1H)			
	^{13}C-NMR chemical shifts (ppm)								
	C=O	H$_2$N-CH$_2$-C<u>H</u>$_2$-	H$_2$N-C<u>H</u>$_2$-CH$_2$-	-CO-NH-C<u>H</u>$_2$-C<u>H</u>$_2$-NH-CO-				-CH$_2$-C<u>H</u>$_2$-C<u>H</u>$_2$-CH$_2$-	
ADC2°	177.0 (s)	41.4 (s)	39.9 (s)	38.7 (s)				35.5 (s)	

*The spectrum was acquired in D_2O at 399.921 MHz; ^The spectrum was acquired in A113 at 299.949 MHz; ° The spectrum was acquired in D_2O at 100.571 MHz

Table 3 Characteristic ^{19}F-NMR chemical shifts of the synthesized products

Product	^{19}F-NMR chemical shifts (ppm)			
	-O-C<u>F</u>$_2$-CONH-	-CF(C<u>F</u>$_3$)-CONH-	-C<u>F</u>$_2$-O-CF$_2$-CONH-	-O-CF$_2$-C<u>F</u>(CF$_3$)-O-
FAD*	-77.3 (s, 2F)	-81.3 (s, 3F)	-86.5 (m, 2F)	-145.9 (m, 1F)
DC6^	-75.8 (s, 2F)	-82.6 (s, 3F)	-85.1 (m, 2F)	-132.3 (m, 1F)
DC2^	-75.6 (s, 2F)	-82.6 (s, 3F)	-85.5 (m, 2F)	-132.2 (m, 1F)

* The spectrum was acquired in CD_3OD at 376.5 MHz; ^The spectrum was acquired neat at 282.203 MHz.

2.3 Products characterization

A Perkin Elmer (Spectrum 1000) Spectrometer was used to record the FT-IR spectra. Two types of supporters for analytes were adopted: the potassium bromide (KBr) windows and the diamond anvil cell. All spectra were recorded in the mid-IR range (4000 cm^{-1} to 400 cm^{-1}). A resolution of 2 cm^{-1} and 16 scans was used for liquid and semi-solid samples on KBr windows. Whereas, a resolution of 2 cm^{-1} and 64 scans were used for rigid samples on the diamond anvil cell.

^{1}H- and ^{13}C-NMR spectra were obtained with a Varian VXR400 (or Varian VXR300) spectrometer operated at 399.921 (or 299.949) MHz and 100.571 MHz respectively, while ^{19}F-NMR spectrum was obtained with a Bruker Avance III (or Varian VXR300) spectrometer operated at 376.5 (or 282.203) MHz. ^{1}H-NMR and ^{13}C-NMR shifts are reported in ppm relative to tetramethylsilane (TMS) at 0 ppm, and ^{19}F-NMR shifts are reported in ppm in respect to $CFCl_3$ at 0 ppm.

2.4 Stone materials

Samples of two lithotypes, Lecce stone and marble (Fig. 1), were selected based on four sequences of water absorption tests previously conducted under the guidance of Norm UNI-EN 15801-2010 [22]. Specimens that demonstrated the most constant water absorptivity (amount of water absorbed within a certain time range, typically 60 min and 120 min) were chosen for subsequent treatment and tests. Lecce stone, widely used mainly in South Italy, is a kind of biocalcarenite. It has a rough, beige surface, characterized by homogeneous and fine grains (grain size distribution between 100 and 200 μm) between which microfossils are commonly seen. The water porosity is around 36-47%, with pore size ranging from 0.1- 2 μm [23, 24]. The Lecce stone samples were previously cut in dimension 5*5*2 cm^3. Carrara marble, quarried from north Tuscany in Italy, has been extensively employed for construction since ancient times. Its main mineralogical constituent is calcite ($CaCO_3$) associated with small percentages of accessory minerals which influence color and veining. The water porosity is about 2%, with pore size distributing from 0.0001- 1 μm [25]. Marble samples are also in dimension 5*5*2 cm^3. For performance testing, three samples of each lithotype were used for each product treatment together with other three samples serving as references.

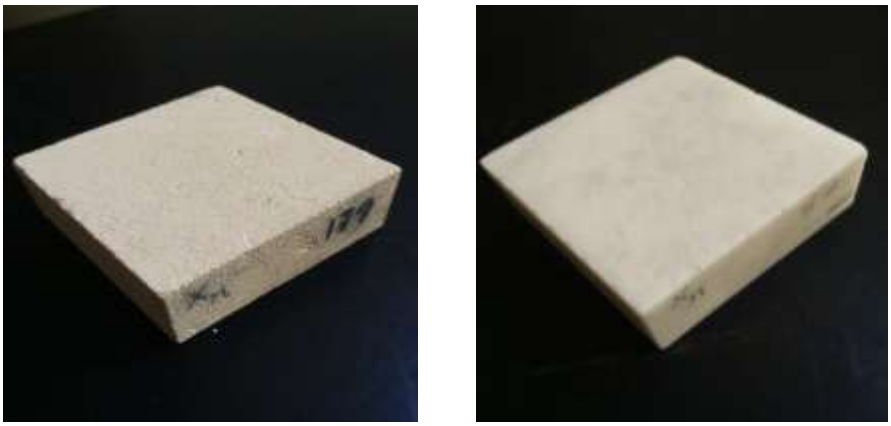

Lecce stone Carrara marble

Figure 1 Stone samples used for performance testing

2.5 Treatments

1% (w/w) FAD/2-propanol solution was prepared at disposal. Solutions of DC2 and DC6 were prepared by using a mixture 90/10 of A113/2-propanol as solvent, with a concentration 10% (w/w) for Lecce stone treatments. The non-functionalized oil of PFPE (YR) was used as neat. For comparison purposes, the commercial fluoroelastomer N215 (1% w/w in acetone) was also applied and tested. Treatments of FAD, N215, DC2, DC6 and YR were all done by using a pipette with the method "wet on wet". The same face used for water capillary absorption test was treated. To start, a suitable amount of solution, e.g., 1 ml was first distributed on the targeted face homogeneously and gently by a pipette. Subsequent additions were made once all liquid was absorbed. Application continued in this way till saturation. The quantities of FAD and N215 to be applied were determined based on the concept obtaining good hydrophobic effect without over saturation. These quantities were preliminarily determined as 20 g/m^2 and 5 g/m^2 for Lecce stone and marble samples, respectively. In the cases of treatments with DC2, DC6 and YR, the amount applied on Lecce stone was determined in 150 g/m^2, while on marble was 15 g/m^2. In both lithotypes the quantity of DC2, DC6 and YR to be applied was higher than that of FAD and N215. For the comparison of the performance of FAD with the other compounds, the less favorable condition, referred to the amount of product required for a decent protective effect, was considered more relevant for the goal. Therefore DC2, DC6 and YR were applied only on Lecce stone. The specific amount of each product applied is reported in Table 4. All samples (including the references) were left under a fume hood at room temperature for one week before performance evaluation.

Table 4 Products amount applied on Lecce stone and Marble

Protective agent	Amount of product (g/m^2)			
	Lecce stone		Marble	
	Theoretical	Actual	Theoretical	Actual
FAD (1% 2-propanol solution)	20	15	5	0.4
N215 (1% acetone solution)	20	14	5	0.4
DC2 (10% A113/2-propanol : 90/10)	150	154	-	-
DC6 (10% A113/2-propanol : 90/10)	150	150	-	-
YR	150	159	-	-

2.6 Treatments evaluation

2.6.1 Water repellence

The water repellency of the products applied was determined in accordance to Norm UNI-EN 15801-2010 [22]. The capillary absorption was considered to demonstrate the hydrophobic properties of compounds applied and the protective efficacy (PE%) was

calculated as:

$$PE\,\% = \frac{A_0 - A_1}{A_1}.100$$

where A_0 and A_1 are the amount of water absorbed before and after treatment.

2.6.2 Vapor permeability

The vapor permeability of treated stone samples was evaluated by the "Cup" method according to Norm UNI-EN 15803-2010 [26].

The "cup" was placed in a closed PVC container at lab temperature (25 °C) and controlled humidity (5% by silica gel). It was weighed at every 24 hours to record the change in weight as the function of time (typically 7 days).

One specimen for each treatment and other three reference specimens of each lithotype were used for vapor permeability test.

Residual permeability percentage (RP%) is calculated according to the formula:

$$RP\,\% = \frac{P_1}{P_o}.100$$

where P_0 is the average permeability of untreated specimens, while P_1 is the permeability of treated ones. The permeability P_0 and P_1 are calculated by the ratio between the weight change of "cup" between two successive measurements (24 hours) and the surface of the sample:

$$P_0 = \frac{\sum_{i=1,2.3}^{i} \frac{\Delta m_i}{s}}{3} \qquad P_1 = \frac{\Delta m_1}{s}$$

where Δm_i is the weight change of "Cup" in which there were the untreated specimens in 24 hours before treatment; Δm_1 is the weight change of the "Cup" containing treated specimens in 24 hours; "s" is the free surface of the specimen through which vapor passes from the inside to outside.

2.6.3 Contact angle

Contact angle of coated and uncoated marble and Lecce stone samples were measured to investigate the wetting properties of coating materials. A Ramè-Hart Model 190 CA Goniometer was employed to measure the static contact angle of 5 µl sessile droplets of distilled water on stone surfaces. For each treatment two specimens were tested, and five measurements were done on each specimen. The contact angle is the average value and it was not corrected on the basis of the stone surface roughness. All measurements were done after the capillary absorption test.

2.6.4 SEM-EDX analysis

The surface morphology of neat and FAD treated Lecce stone samples was characterized by an environmental scanning electron microscopy (mod. ESEM Quanta – 200 FEI) equipped with an energy - dispersive x-ray spectrometer (X-EDS). Images in secondary (LFD) and backscattered (SSD) electron were acquired, and elemental composition was obtained working at pressure of 0.50 and 0.25 Tor with a voltage of 25 KeV.

2.6.5 Chromatic effect

On the basis of Norm UNI-EN 15886-2010 [27], chromatic changes of stone surfaces induced by protective coatings were evaluated by colorimetric analysis conducted before and after polymer applications. A portable spectrophotometer X-Rite SP60 was used and a SPEX (specular component excluded) model was adopted.

For each sample, 3 measurements were performed on each spot previously selected and located by using a mask. Results were elaborated on the basis of chromaticity coordinates and reported in CIE-L*a*b* standard color system: for each defined spot on a sample the average value of L*a*b* was used, where L* indicates the brightness and ranges from 0 (black) to 100 (white); a* and b* are the color axes and their values range from -60 to +60. On the a* axis, positive values indicate amount of red, whereas the negative ones indicate green. On the b* axis, yellow is positive while blue is negative. The color alterations were evaluated by the difference of the vector E* (ΔE), expressed as:

$$\Delta E = \sqrt{\Delta L^{*2} + \Delta a^{*2} + \Delta b^{*2}}$$

where ΔL*, Δa* and Δb* are the value differences before and after treatment. The value ΔE* = 3 is commonly regarded as the detection limit of human eyes and samples that have a ΔE* value less than or equal to three implies an imperceptible chromatic change [28].

3. Results and discussion

3.1 Synthesis and characterization of non-fluorinated oligoadipamide

The synthesis was realized via poly-condensation reaction (Scheme 2). Instead of using acid, ester of dicarboxylic acid was used to avoid salt formation which requires higher temperature for amide formation. Aiming at obtaining oligoamide with terminal amine groups for successive reactions, the molar amount of ethylenediamine was kept in excess. Synthesis with different molar ratios between ethyl adipate and ethylenediamine (1:5, 1:3 and 1:2), and reactions with or without solvent, were also tried (Table 5). After 60 hours, no pure oligoadipamide was obtained for the reactions with ratios 1:3 and 1:2 due to the unreacted ethyl adipate. Problems may arise from inadequate stirring, heating or solvent presence which creates difficulties for the approaching of ethylenediamine, and consequently, one ester group in the molecule was left unreacted. Extracted and purified by diethyl ether for 5 times, the suspicious compound was proved to contain unreacted ethyl adipate. In the FT-IR spectrum, only one peak of C=O stretching group disappeared while the other peak at 1731 cm^{-1} was still present (Fig. 2). Finally, reaction conditions with molar ratio 1:5 (ethylenediamine in large excess), higher reaction temperature (95-100 °C) and solvent free gave rise to good yield of product in 22 hours. The final product (ADC2) showed good solubility in water and partial solubility in alcoholic solvents (Table 6), and its molecular weight (M_n) was determined to be 296 g/mol.

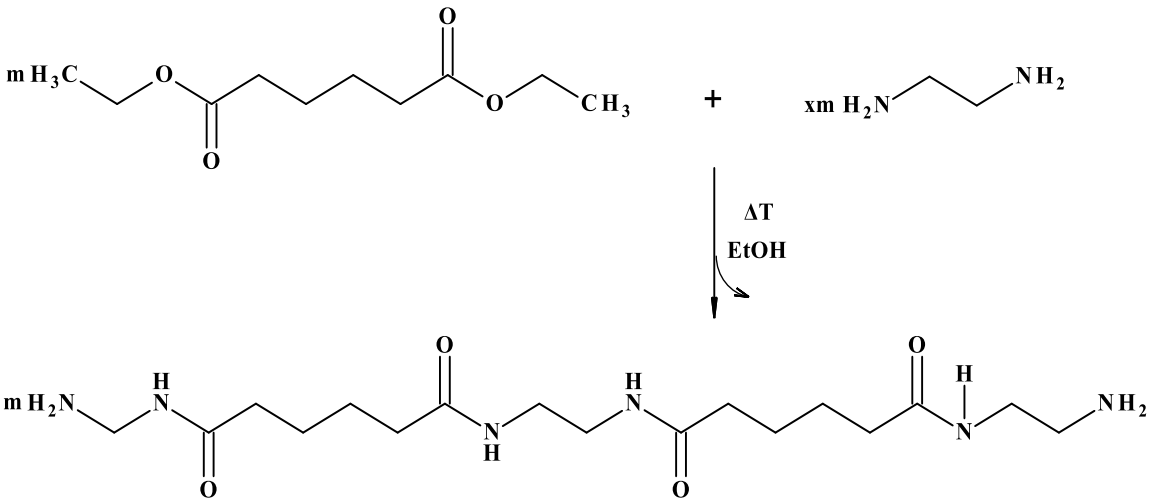

where x= 2, 3, 5.

Scheme 2 Synthesis of non-fluorinated oligoamide

Table 5 Reaction conditions of oligoadipamide syntheses

R#	Ethylene-diamine g (mmol)	Ethyl adipate g (mmol)	Solvent THF (ml)	T. (°C)	Time (h)	Yield (%)
ADC2-1	0.51 (9.90)	1.00 (4.95)	2	80-85	60	0
ADC2-2	0.77 (14.85)	1.00 (4.95)	2	80-85	60	0
ADC2	1.28 (24.75)	1.00 (4.95)	0	95-100	22	61

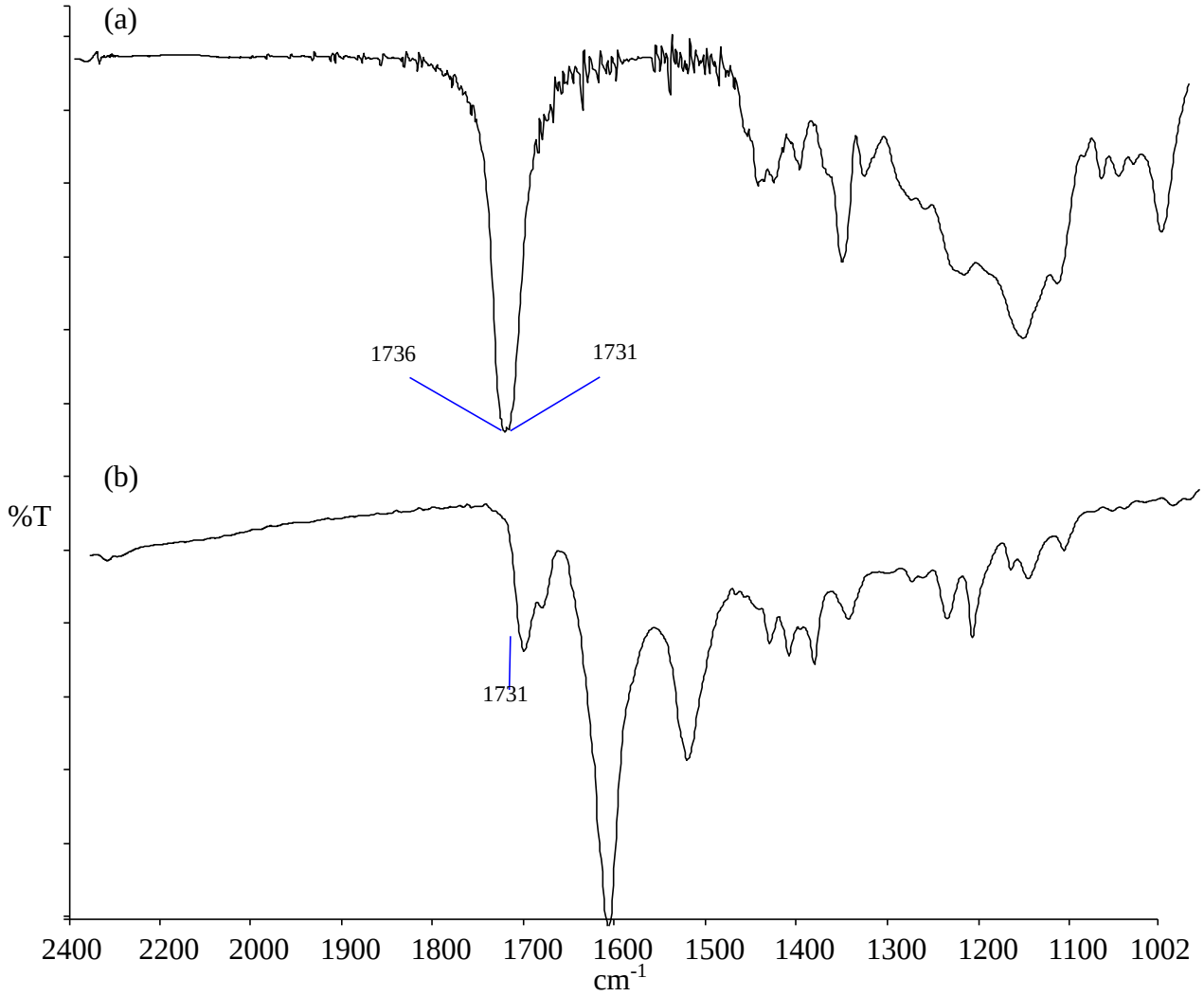

Figure 2 FT-IR spectra (on KBr windows) of diethyl adipate (a) and ADC2-2 (b)

Table 6 Solubility of ADC2 determined as percentage of product dissolved in a mixture containing 1% (w/w) of amide in solvent

Solvent	Solubility (%)	
	Cold (20-25°C)	Hot (80-90°C)
H_2O	100	100
THF	0	n.d.
2-propanol	15	80
Diethyl ether	0	n.d.

^{1}H-NMR spectroscopy was used to estimate the M_n of ADC2. Indeed, this technique is not only a powerful tool for molecular characterization, but also a valid method to elucidate polymer structures, including the molecular weight [29]. The calculation method here used was able to characterize not only the number-average molecular weight but also the molecular weight distribution. Referring to the theoretical formula of ADC2 (Scheme 3), the proton signals in the ^{1}H-NMR spectrum (Fig. 3) could be easily assigned.

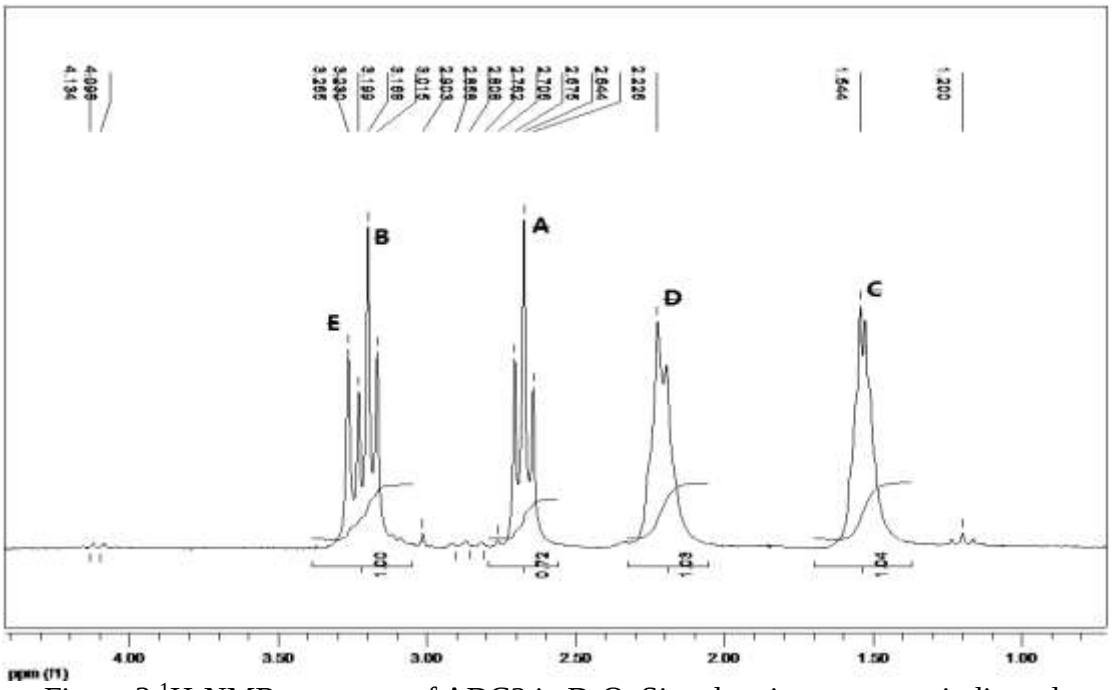

Figure 3 ^{1}H-NMR spectrum of ADC2 in D_2O. Signal assignments are indicated.

H_2N-CH_2-CH_2-NH-CO-CH_2-$(CH_2)_2$-CH_2-CO-[HN-CH_2-CH_2-NH-CO-CH_2-$(CH_2)_2$-CH_2-CO]$_p$-NH-CH_2-CH_2-NH_2

where p is the polymerization degree (Scheme 3)

When p=0:

H_2N-CH_2-CH_2-NH-CO-CH_2-$(CH_2)_2$-CH_2-CO-NH-CH_2-CH_2-NH_2

A B D C D B A

When p=1:

H_2N-CH_2-CH_2-NH-CO-CH_2-$(CH_2)_2$-CH_2-CO-NH-$(CH_2)_2$-NH-CO-CH_2-$(CH_2)_2$

A B D C D E D C

-CH_2-CO-NH-CH_2-CH_2-NH_2

D B A

When p =2:

H_2N-CH_2-CH_2-NH-CO-CH_2-$(CH_2)_2$-CH_2-CO-NH-$(CH_2)_2$-NH-CO-CH_2-$(CH_2)_2$

A B D C D E D C **-CH_2-CO-HN-$(CH_2)_2$-NH-CO-CH_2-$(CH_2)_2$- CH_2-CO-NH-CH_2-CH_2-NH_2**

D E D C D B A

When p=3;4 and so on…

The corresponding signal assignments are:

i. Singlet at 3.27 ppm (E) attributes to protons of 2 methylene groups adjoining 2 amidic groups in the middle of chain: CO-NH-C$\underline{H}_2$-C$\underline{H}_2$-NH-CO, for p≥1;

ii. Triplet at 3.20 ppm (B) attributes to protons of methylene group in β position of the terminal amino group: NH_2-CH_2-C$\underline{H}_2$-NH;

iii. Triplet at 2.67 ppm (A) attributes to protons of methylene group in α position of the terminal amino group: H_2N-C$\underline{H}_2$;

iv. Singlet at 2.23 ppm (D) attributes to protons of 2 methylene groups in α position of 2 carbonyl groups: NH-CO-C$\underline{H}_2$-$(CH_2)_2$-C$\underline{H}_2$-CO-NH;

v. Singlet at 1.54 ppm (C) attributes to protons of 2 methylene groups in β position of 2 carbonyl groups: NH-CO-CH_2-C$\underline{H}_2$-C$\underline{H}_2$-CH_2-CO-NH;

Since the integral of signal area is proportional to the number of protons, the number of each type of protons is countable based on the following equations:
Protons of group A: $\int_{Signal\ A}$ =0.72 ascribing to 4H;
Protons of group B: $\int_{Signal\ B}$ =0.72 ascribing to 4H;
Protons of group C: $\int_{Signal\ C}$ =1.04 ascribing to 4H·(p +1);
Protons of group D: $\int_{Signal\ D}$ =1.03 ascribing to 4H·(p +1);
Protons of group E: $\int_{Signal\ E}$ =0.28 ascribing to 4H· (p).

Presuming there is m mol of oligomers with p=0, n mol of oligomers with p=1 and s mol of oligomer with p=2, t mol of oligomer with p=3, the following equations are built:

$0.72 = m + n + s$ (Eq. 1)
$0.72 = m + n + s$ (Eq. 2)
$1.04 = m + 2n + 3s$ (Eq. 3)
$1.03 = m + 2n + 3s$ (Eq. 4)
$0.28 = n + 2s$ (Eq. 5)

It shall be noticed that when p=3, there are four unknown variables (m, n, s, t), but in this case only 3 equations can be written, indicating "t" does not exist. Solving these equations, "m", "n", and "s" are 0.5, 0.16 and 0.06 respectively. The corresponding proportions of oligomers with these 3 chain lengths are computable, being 69.4% (p=0), 22.2% (p=1) and 8.3% (p=2) respectively. Therefore, the number-average molecular weight is:

$$M_n = \frac{\sum_{i=1,2.3}^{i} n_i \bullet M_i}{\sum_{i=1,2.3}^{i} n_i} = (0.5 * M_{ADC2p=0} + 0.16 * M_{ADC2p=1} + 0.06 * M_{ADC2p=2}) / 0.72 =$$

$(0.5*230 + 0.16*400 + 0.06*570)/ 0.72=296.11.$

$$M_w = \frac{\sum_{i=1,2.3}^{i} n_i \bullet M_i^2}{\sum_{i=1,2.3}^{i} n_i \bullet M_i} = (0.5*230^2 + 0.16*400^2 + 0.06*570^2)/ (0.5* 230 +0.16*400 +$$

$0.06*570) = 335.57.$

Polydispersity = D= M_w/M_n = 1.1.

3.2 Synthesis and characterization of partially fluorinated oligoadipamide and C2 and C6 diamides

In FAD synthesis, perfluoropolyetheric segments were grafted to the two ends of oligoamides (Scheme 4).

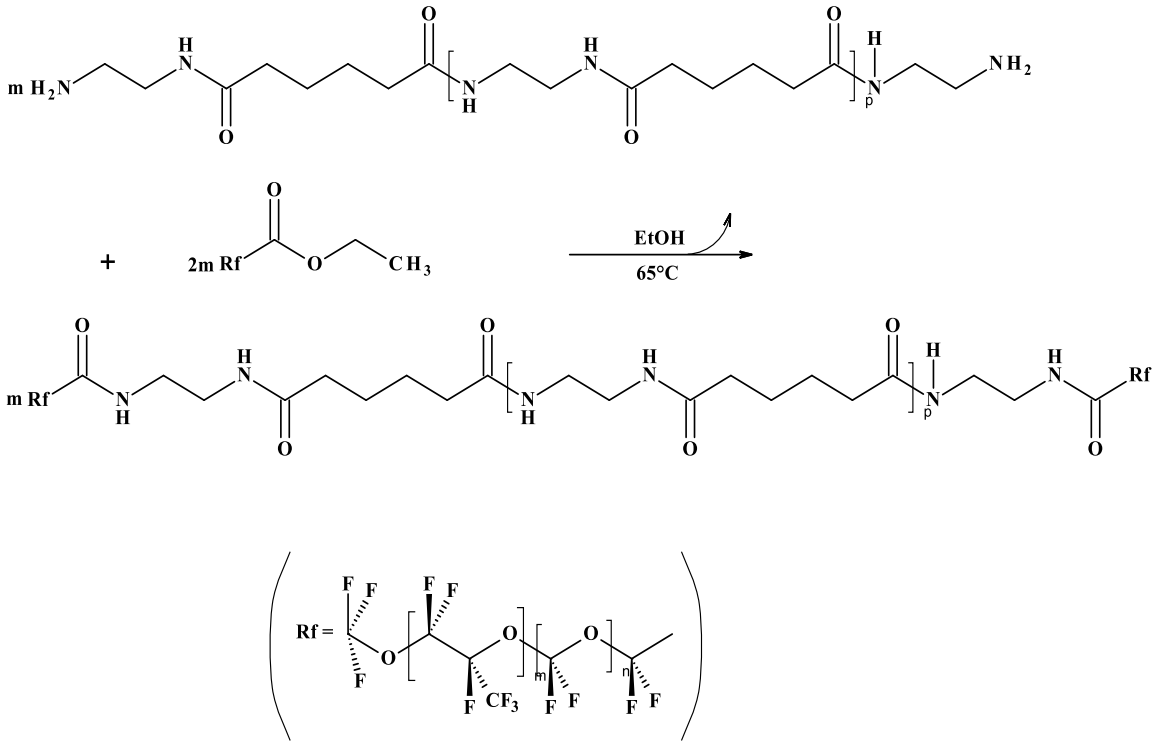

Scheme 4 Synthesis of partially fluorinated oligoamide

Based on the M_n of ADC2 found by ^{1}H-NMR, the molar ratio ADC2:PFPE (1:2) was adopted (Table 7). The conversion of ADC2 into FAD was considered completed when the peak height of C=O stretching of PFPE ester in the FT-IR spectrum (1792 cm^{-1}) tended to zero, while the peak height ratio between C=O stretching of fluorinated amide (1705 cm^{-1}) and C=O stretching of not fluorinated amide (1641 cm^{-1}) remained constant (Fig. 4).

The insertion of two highly fluorinated segments influenced the main absorption bands of non-fluorinated oligoamide. The peak of C=O stretching (amide I) shifted from 1637 to 1641cm^{-1}, the N-H bending from 1554 to 1559 cm^{-1}, and the N-H symmetric stretching and C-H stretching also experienced shifting from 3082 and 2938 cm^{-1} to 3089 and 2949 cm^{-1}, respectively. The N-H asymmetric stretching, nonetheless, remained steady (3295-3296 cm^{-1}).

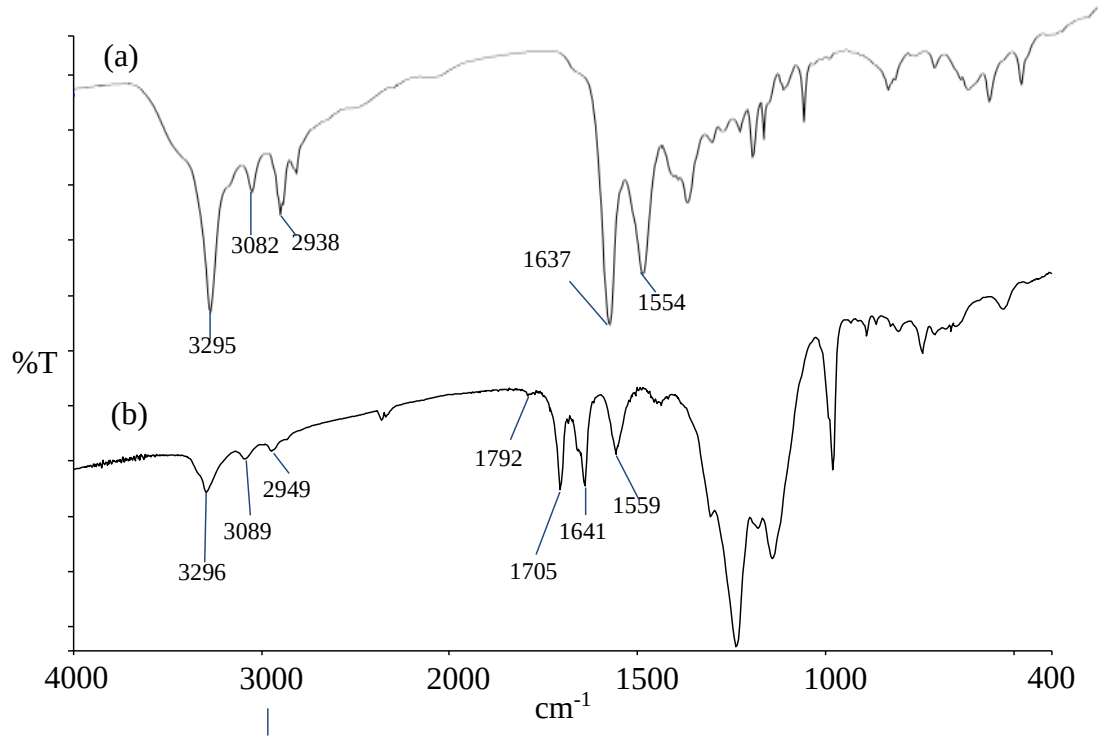

Figure 4 FT-IR spectrum of ADC2 (a) and FAD (b) on KBr windows

The syntheses of DC2 and DC6 went smoothly (Scheme 5), and high yields were achieved in mild conditions (Table 7). However, difficulties appeared when it came to purification, since neither distillation nor recrystallization or sublimation work well for these oily diamides. Another tentative purification method was tried by using a column of silica gel, but it had problems for product recovery. Eluents with less polarity were not able to move the amides from the support, while more polar eluents recover the amide together with its decomposed byproducts. The method with the best accuracy and reproducibility were treatments with active carbon, giving rise to colorless, heat-stable products.

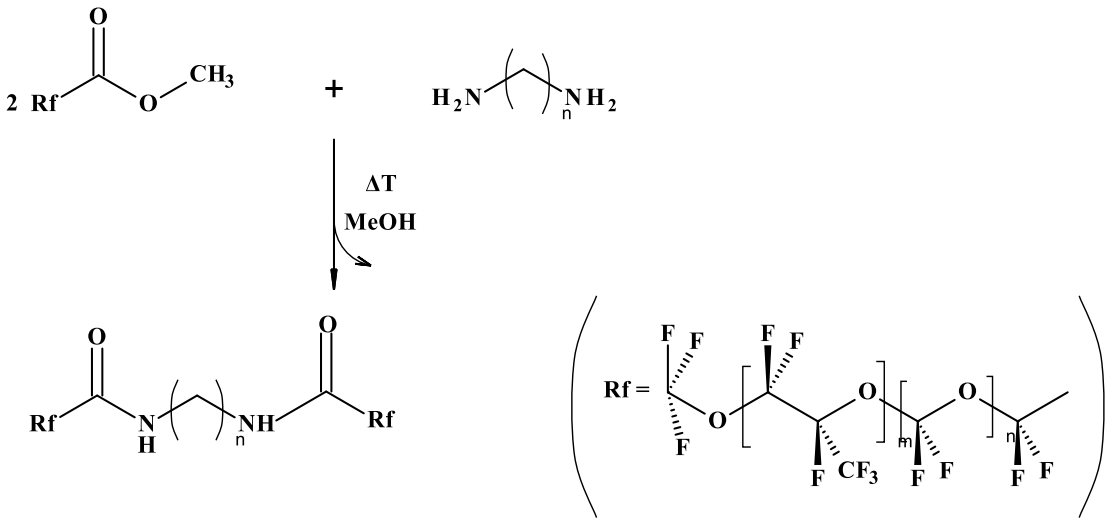

where n= 2, 6.

Scheme 5 Synthesis of ethylene- and hexamethylene-diamides (DC2 and DC6)

Table 7 Reaction conditions used in the synthesis of FAD, DC2 and DC6

Product	Reagents (g) (mmol)					Solvent (ml)	Temp. (°C)	Time (hours)	Yield (%)
	ADC2	C2	C6	EtG	MetG				
FAD	0.15 (0.51)			0.89 (1.02)		5*	65	40	95
DC2		0.48 (8.00)			14.50 (16.11)	10**	Room T	4	99
DC6			0.49 (4.20)		7.70 (8.50)	10**	Room T	6	95

C2 = ethylenediammine; C6 = hexamethylenediammine; EtG = Ethyl ester of Galden acid; MetG = methyl ester of Galden acid; *2-propanol; ** A113

The different structure and length of non-fluorinated chain have influence on the solubility of oligoamides (Table 8). FAD has the best solubility in alcoholic and hydro-alcoholic solvents, while DC2 and DC6 are mainly soluble in chlorofluorocarbons. The slightly higher molecular weight of FAD than DC2 and DC6 (Table 9) is due to the relatively longer alkyl chain of the oligoadipamide. This chain, with good chemical affinity towards common organic solvents, is able to balance the poor affinity of PFPE blocks, giving rise to better solubility in alcoholic solvents than DC2 and DC6. On the contrary, the chemical and physical properties of DC2 and DC6 are predominantly determined by the PFPE segments.

Table 8 Solubility of FAD, DC2 and DC6 determined as percentage of amide dissolved in a mixture containing 1% (w/w) of product in solvent

Solvent	FAD		DC2		DC6	
	Cold	Hot	Cold	Hot	Cold	Hot
Ether	0	n.d.	80	n.d.	80	n.d.
Ethanol	90	100	n.d.	n.d.	n.d.	n.d.
2-propanol	80	100	10	50	10	50
2-propanol/ H_2O (70:30)	50	90	0	n.d.	0	n.d.
A113	0	n.d.	100	n.d.	100	n.d.
A113/ 2-propanol (90/10)	n.d.	n.d.	100	n.d.	100	n.d.
A113/ 2-propanol (10/90)	n.d.	n.d.	30	n.d.	30	n.d.
Ethanol	100	n.d.	n.d.	n.d.	n.d.	n.d.
2-propanol	100	n.d.	50	n.d.	50	n.d.
2-propanol/ H_2O (70:30)	90	n.d.	n.d.	n.d.	n.d.	n.d.

Cold = 20-25°C; Hot = 60-65°C

Table 9 Number-average molecular weight of FAD, DC2 and DC6 calculated and found by viscometry

Product	M_n (calculated)	M_n (by Viscometry [18])
FAD (PFPE-Oligoadipamide-PFPE)	2096 (^{1}H-NMR)	-
DC2 (PFPE-CO-NH-CH_2-CH_2-NH-CO-PFPE)	1785	1612
DC6 (PFPE-CO-NH-CH_2-CH_2-CH_2-CH_2-CH_2-CH_2-NH-CO-PFPE)	1840	1341

3.3 Treatments evaluation

The performance of fluorinated oligoamides were tested on marble and/or Lecce stone. In Figure 5, the change of wettability of the stone surface after coating with FAD is shown as example. To compare the hydrophobic properties of synthesized products and the commercial products (N215 and YR), the protective efficacy was tested on Lecce stone and reported in Table 10. The protective efficacy (PE%) after 30 minutes of water absorption was comparable for all the products, except for YR, the non-functionalized perfluoropolyether. However, only FAD and N215 showed good hydrophobicity with very low amount of product (10 times lower than DC2, DC6 and YR).

Table 10 Protective efficacy (PE%) on Lecce stone of some fluorinated compounds

after 30-minutes of water absorption		
Treatment	Amount of product applied (g/m^2)	PE% 30 min
FAD	15	79
DC2	154	70
DC6	150	86
YR	159	33
N215	14	75

(a) (b)

Figure 5 Marble samples before (a) and after (b) coating with FAD

Concerning the long-time protective efficacy of FAD, evaluations were done by comparing performance with N215. As reported in Table 11, FAD and N215 have exhibited similar hydrophobic effects when tested on Lecce stone, with good but not excellent reduction of water uptake. On the contrary, on marble samples, coated with the same amount of product, conspicuously high PE% (≥ 90%) values were obtained with FAD, both at short time (30 minutes) and long time (4 hours). The fluoroelastomer, on the other hand, showed lower PE% values which, after 4 hours of water absorption, were 3 times lower than the treatment with FAD.

Table 11 Protective efficacy (PE%) of FAD, N215 coated stone samples at different time of water absorption

Treatment	Stone	Concentration (g/m^2)	PE%* at				
			30 min	60 min	120 min	180 min	240 min
N215	Lecce stone	14	75	66	48	-	-
	marble	0.4	-	56	46	39	30
FAD	Lecce stone	15	79	67	44	-	-
	marble	0.4	-	94	92	90	90

* = PE% was calculated as the mean value of two absorption tests

The different behavior of FAD in the efficiency of water absorption inhibition when applied on marble or Lecce stone can be justified on the basis of the physical-chemical properties of FAD, and of the porous structure (typically porosity and pore size) of these stones. The FAD chains, derived from low polymerized oligoadipamide, have linear and polar internal segments able to interact by predominant intermolecular hydrogen bonding between -NH and -C=O groups. In dilute solution, such as that used for the stones treatment, the intermolecular interactions are drastically reduced and the polar groups are available to interact with the polar substrate. Thanks to the dilute solution a uniform distribution of FAD on the surface is expected, where the amidic chains are anchored to the stone while the perfluorinated blocks act at the stone/air interface giving the hydrophobic effect. When the substrate has a low porosity (i. e. marble, porosity about 2%, pore size 0.0001- 1 μm) all the product is mainly distributed on the external surface providing high hydrophobic efficiency. On the contrary, when the stone has high porosity (i.e. Lecce stone, porosity up to 45-47%, pore size 0.1- 2 μm) the dilute solution of FAD can diffuse inside the substrate reducing the actual quantity of product for surface unit. This means that the amount of 15 g/m^2 calculated from the mass of FAD applied on the 5x5 cm^2 surface can be drastically reduced. Therefore, even if the product has excellent hydrophobic properties, the water uptake cannot be completely stopped. In support of this hypothesis the contact angle measurements gave us useful information, and high values were found, both on marble and Lecce stone (Fig. 6). However, in the case of marble, where the penetration of the coating agents is expected very low and comparable amount of product are actually deposed on the detected surfaces, higher contact angle for FAD (120±2°) than for N215 (89±4°) was found. On the contrary, on Lecce stone similar contact angle for FAD (114±7°) and N215 (113±2°) was observed because of the different penetration of the two products. Indeed, the larger molecular size of N215 (Mw 125,000) in respect to FAD (Mn 2100) and the higher vapor pressure of the solvent used (acetone, vp@20°C = 184 mmHg, against 2-propanol, vp@20°C = 33 mmHg) inhibit a high penetration of the fluoroleastomer giving rise to an accumulation of the coating agent on the external surface.

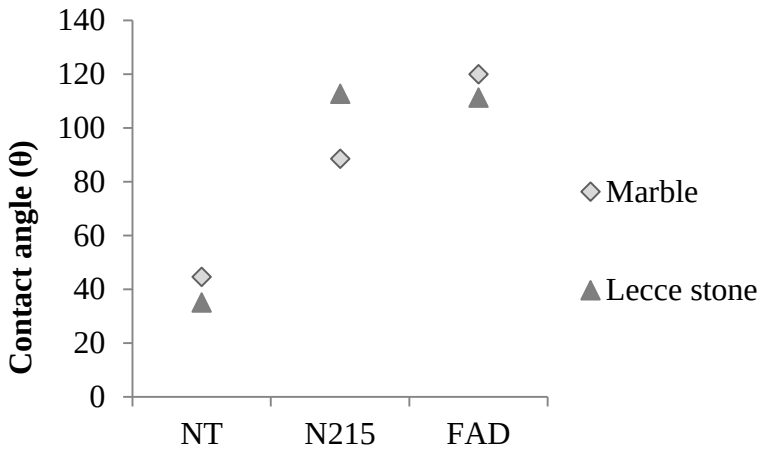

Figure 6 Contact angle of neat and treated stone samples

In addition to the high protective efficacy, the original vapor permeability of marble and Lecce stone was only slightly decreased, both for FAD and N215 treatments (Table 12). The RP% values were always higher than 80%.

These results are in agreement with the surface morphology observed by SEM. Indeed, the microstructure of the stones was not modified after coating. In Figs. 7-10 some SEM-LFD (Large Field detector) micrographs of Lecce stone, neat and coated with FAD, are shown as examples. Nevertheless, the presence of the fluorinated compound was detected by EDX microanalysis (Fig. 11).

Table 12 Residual permeability (RP%) of stone samples after coating

Treatment	Stone type	Concentration (g/m^2)	RP%
FAD	Lecce stone	15	90
	marble	0.4	89
N215	Lecce stone	14	87
	marble	0.4	91

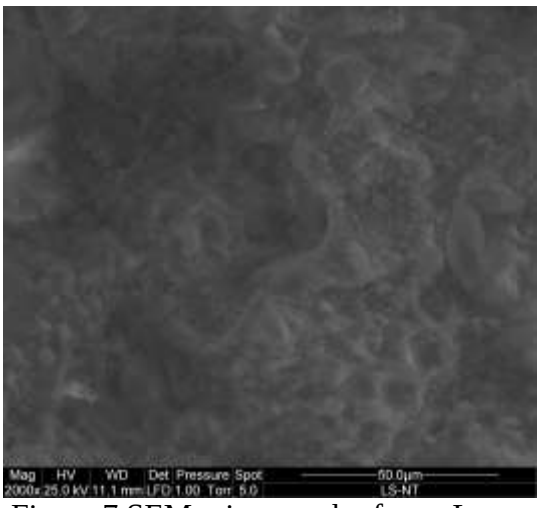

Figure 7 SEM micrograph of neat Lecce stone (2000x)

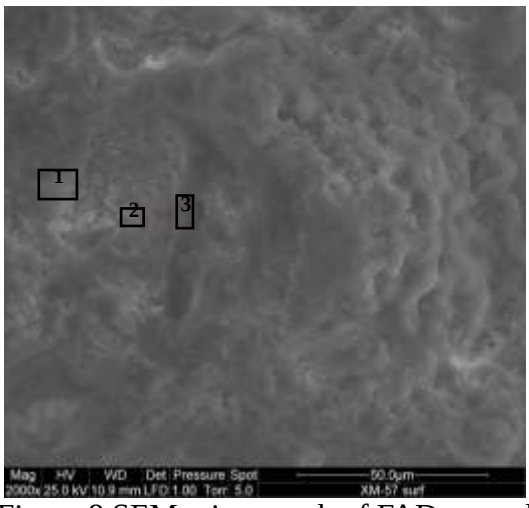

Figure 8 SEM micrograph of FAD treated Lecce stone (2000x)

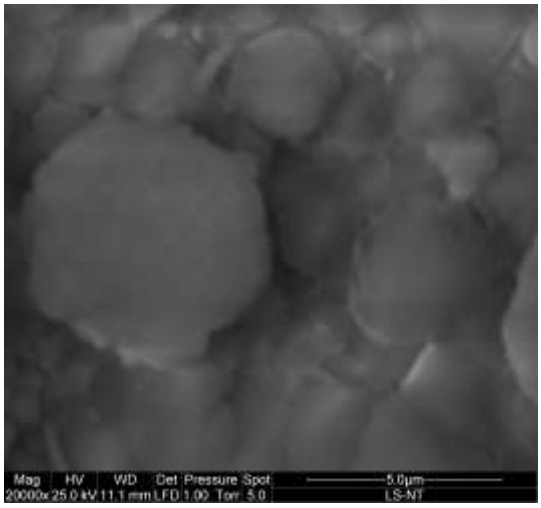

Figure 9 SEM micrograph of neat Lecce stone (20000x)

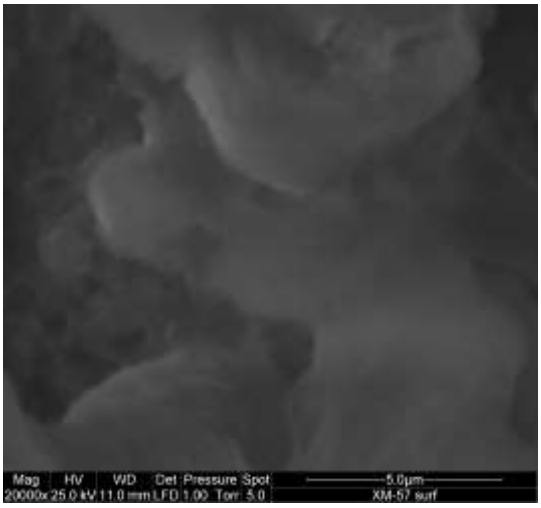

Figure 10 SEM micrograph of FAD treated Lecce stone (20000x)

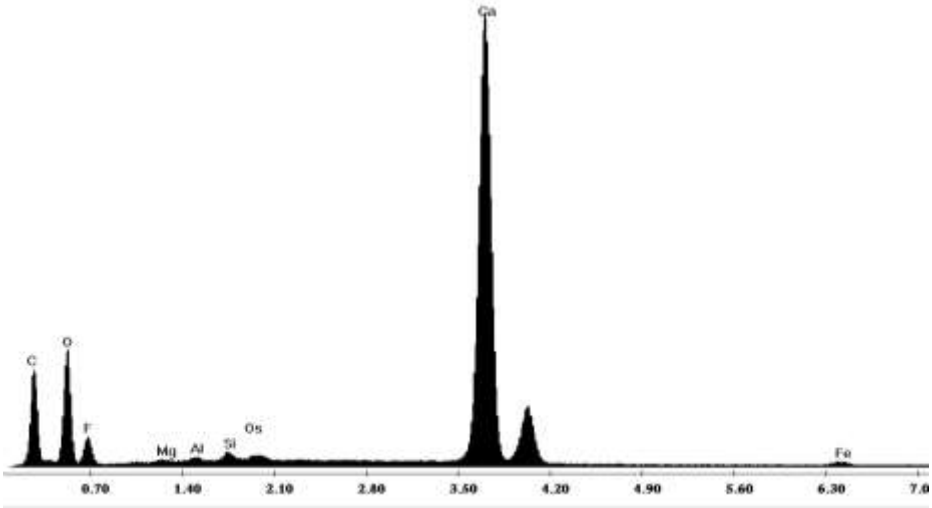

Figure 11 EDX analysis of Area 1 in Figure 8

Moreover, no appreciable chromatic changes were observed on stone surfaces treated with FAD and N215 (Fig. 12), since the chromatic variations were below the detect limit of human eyes ($\Delta E=3$) [28].

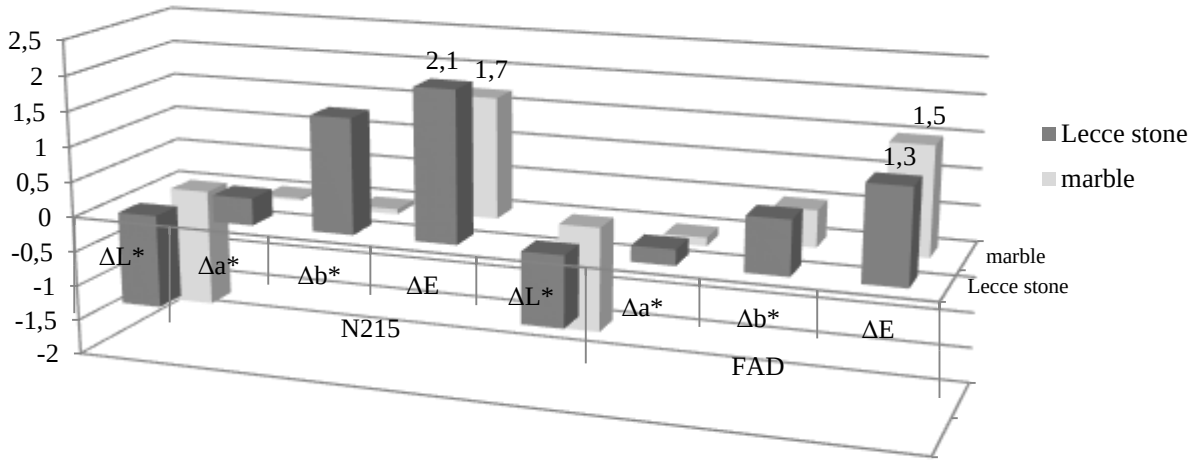

Figure 12 Color variations of stone surfaces after coating

4. Conclusions

In this work, a new oligoadipamide incorporating highly hydrophobic PFPE pendant segments and two diamides with PFPE blocks were synthesized. The oligoadipamide (FAD) has good solubility in alcohols and hydro-alcoholic solvents e.g. ethanol, 2-propanol, while the two diamides are only soluble in chlorofluorocarbons. Solubility in common solvents is of vital importance for the wide application of protective coatings, and additionally, using alcoholic or hydro-alcoholic solvents, FAD treatments are not only healthy to human beings but also environmentally friendly. Despite of the solubility limit, the number-average molecular weight and molecular weight distribution of FAD were wisely elucidated by exploiting ^{1}H-NMR spectroscopy. Their performances as protective coatings were tested as well. FAD has manifested much higher hydrophobicity than the other products, though the amount applied was, in some cases, much lower. When applied on marble FAD showed the best performance, while on Lecce stone it gave similar hydrophobic effect than the fluoroelastomer N215 attributing to its higher propensity, during the application, to diffuse inside the porous substrate. In addition, FAD preserved the original microstructure, vapor permeability and chromatic features of coated stone surfaces, fulfilling the prerequisites for conservation intervention on artworks. All results indicate the potential use of FAD as a protective coating for low porous stone materials, including stone artworks.

Further studies are in progress in order to verify the stability and long-term performance durability of FAD protective coating, by means of chemical, thermal and photo-oxidative ageing tests and field exposure tests.

Acknowledgement

The authors would like to thank Prof. Rodorico Giorgi and Dr. Martina Raudino (Department of Chemistry and CSGI, University of Florence) for help with the contact angle measurement.

References

[1] E. Doehne, C. A. Price, Stone Conservation: An Overview of Current Research, 2nd ed,; The Getty Conservation Institute: Los Angeles, 2010, ISBN: 978-1606060469.

[2] C. Sabbioni, Contribution of atmospheric deposition to the formation of damage layers, Sci. Total. Environ. 167 (1995) 49-55, http://dx.doi.org/10.1016/0048-9697(95)04568-L.

[3] D. Barca, V. Comite, C. M. Belfiore; C. Sabbioni, Impact of air pollution in deterioration of carbonate building materials in Italian urban environments, Appl. Geochem. 48 (2014) 122-131, http://dx.doi.org/10.1016/j.apgeochem.2014.07.002.

[4] M. M Rosa, W. S. George, Advance in understanding damage by salt crystallization, Acc. Chem. Res. 43 (2010) 897-905, http://dx.doi.org/10.1021/ar9002224.

[5] F. Bayram, Predicting mechanical strength loss of natural stones after freeze–thaw in cold regions, Cold. Reg. Sci. Technol. 83-84 (2012) 98-102, http://dx.doi.org/10.1016/j.coldregions.2012.07.003.

[6] D. Pinna, O. Salvadori, Process of biodegradation: General Mechanisms in G. Caneva, M. P. Nugari, O. Salvadori (Eds), Plant Biology for Cultural Heritage, The Getty Conservation Institute, Los Angeles, 2009, pag. 15-55 (Chapter 2), ISBN 978-0-89236-939-3.

[7] K. Beck, M. Al-Mukhtar, O. Rozenbaum, M. Rautureau, Characterization, water transfer properties and deterioration in tuffeau: building material in the Loire valley—France, Build. Enviro. 38 (2003) 1151-1162, http://dx.doi.org/10.1016/S0360-1323(03)00074-X.

[8] L. Lazzarini, M. Laurenzi Tabasso, Il Restauro della Pietra, Editor: Utet Scienze Tecniche, 2010, ISBN: 978-8859805434.

[9] A. E. Charola, Water-repellent treatments for building stones: A practical overview APT Bulletin 26 (1995) 10-17, http://dx.doi.org/10.2307/1504480.

[10] G. G. Amoroso, M. Camaiti, Scienza dei materiali e restauro-La pietra: dalle mani degli artisti e degli scalpellini a quelle dei chimici macromolecolari, Alinea Ed., Florence, 1997.

[11] R. Striani, M. Frigione, C. E. Corcione, UV-cured siloxane-modified methacrylic system containing hydroxyapatite as potential protective coating for carbonate stones, Prog. Org. Coat. 76 (2013) 1236-1242, http://dx.doi.org/10.1016/j.porgcoat.2013.03.024.

[12] M. Laurenzi. Tabasso, Acrylic Polymers for the Conservation of Stone: Advantages and Drawbacks, APT Bulletin 26 (1995) 17-21, http://dx.doi.org/10.2307/1504445.

[13] M. J. Melo, S. Bracci, M. Camaiti, O. Chiantore, F. Piacenti, Photodegradation of acrylic resins used in the conservation of stone, Polym. Degrad. Stabil. 66 (1999) 23-30, http://dx.doi.org/10.1016/S0141-3910(99)00048-8.

[14] M. Lazzari, M. Aglietto, V. Castelvetro, O. Chiantore, Photochemical stability of partially fluorinated acrylic protective coatings IV. Copolymers of 2, 2, 2-trifluoroethyl methacrylate and methyl α-trifluoromethyl acrylate with vinyl ethers, Polym. Degrad. Stabil. 79 (2003) 345-351, http://dx.doi.org/10.1016/S0141-3910(02)00298-7.

[15] O. Chiantore, M. Lazzari, Photo-oxidative stability of paraloid acrylic protective polymers, Polymer 42 (2001) 17-27, http://dx.doi.org/10.1016/S0032-3861(00)00327-X.

[16] M. Favaro, R. Mendichi, F. Ossola, S. Simon, P. Tomasin, P. A. Vigato, Evaluation

of polymers for conservation treatments of outdoor exposed stone monuments. Part II: Photo-oxidative and salt-induced weathering of acrylic-silicone mixtures, Polym. Degrad. Stabil. 92 (2007) 335-351, http://dx.doi.org/10.1016/j.polymdegradstab.2006.12.008.
[17] F. Piacenti, F. Ciampelli, A. Pasetti, Protecting materials subject to degradation by atmospheric and polluting agents by means of perfluoropolyethers US 4499146 A (1983).
[18] F. Piacenti, M. Camaiti, Synthesis and characterization of fluorinated polyetheric amides, J. Fluo. Chem. 68 (1994) 227-235, http://dx.doi.org/10.1016/0022-1139(93)03045-N .
[19] F. Piacenti, A. Pasetti, U. Matteoli, E. Strepparola, Method for protecting stone materials from atmospheric agents by means of perfluoropolyether derivatives US 4745009 A (1986).
[20] C. E. Circione, R. Manno, M. Frigione, Sunlight-curable boehmite/siloxane-modified methacrylic based nanocomposites as insulating coatings for stone substrates, Prog. Org. Coat. 95 (2016) 107-119, http://dx.doi.org/10.1016/j.porgcoat.2016.03.007.
[21] C. E. Circione, R. Manno, M. Frigione, Sunlight curable boehmite/siloxane-modified methacrylic nano-composites: An innovative solution for the protection of carbonate stones, Prog. Org. Coat. 97 (2016) 222-232, http://dx.doi.org/10.1016/j.porgcoat.2016.04.037
[22] Norm UNI-EN 15801-2010, 2010, “Conservation of Cultural Heritage–Test methods–Determination of water absorption by capillarity”.
[23] S. Bugani, M. Camaiti, L. Morselli, E.V. de Casteele, K. Janssens, Investigation on porosity changes of Lecce stone due to conservation treatments by means of x-ray nano- and improved micro-computed tomography: preliminary results, X-Ray Spectrom. 36 (2007) 316-320, http://dx.doi.org/10.1002/xrs.976.
[24] S. Bugani, M. Camaiti, L. Morselli, E.V. De Casteele, K. Janssens, Investigating morphological changes in treated vs. untreated stone building materials by x-ray micro-CT, Anal. Bioanal. Chem. 391 (2008) 1343-1350, http://dx.doi.org/10.1007/s00216-008-1946-7.
[25] C. G. Borgia, V. Bortolloti, M. Camaiti, F. Cerri, P. Fantazzini, F. Fratini; F. Piacenti, Caratterizazione struttuale di materiali porosi: un nuovo approccio mediante tecniche NMR, Patron Editore, Proceedings of National Archaeometry Congress, Bologna-Italy, 29 January-1 February, 2002, 135-150.
[26] Norm UNI-EN 15803-2010, 2010 “Conservation of Cultural Heritage–Test methods–Determination of water vapor permeability”.
[27] Norm UNI-EN 15886-2010, 2010, “Conservation of Cultural Heritage–Test methods–Measurement of the color of the surface”.
[28] C. M. Grossi, P. Blimblecombe, R. M. Esbert, F. J. Alonso, Color changes in architectural limestones from pollution and cleaning. Color Res. Appl. 32 (2007) 320-331, http://dx.doi.org/10.1002/col.20322.
[29] S.C. Shit, S. Maiti, Application of NMR spectroscopy in molecular weight determination of polymers, Eur. Polym. J. 22(1986) 1001-1008, http://dx.doi.org/10.1016/0014-3057(86)90082-0.